Manuscript for Int. J. of Heat and Mass Transfer (14/11/2007)

Phase-shifted ventilation, a new thermal storage concept for passive cooling of buildings: theoretical and experimental characterization

Pierre Hollmuller *), Bernard Lachal, Jean-Marc Zgraggen
Centre universitaire d'études des problèmes de l'énergie, Université de Genève, CH - 1227 Carouge, Switzerland

*) corresponding author
tel: (+41) 22 / 379 0649
fax: (+41) 22 / 379 0639
e-mail: pierre.hollmuller@cuepe.unige.ch

ABSTRACT

This paper concerns a newly discovered heat storage technique, which uses a thermal storage similar to a packed-bed, of very precise geometry and dimension. Aim is to delay the meteorological oscillation carried by the ventilation airflow – almost without dampening – so as to provide the nightly cooling peak in the middle of the day, for passive cooling of buildings. After description of the physical phenomena, by way of a simple analytical model, we present the development and characterization of a series of prototypes.

KEYWORDS

packed-bed, thermal storage, ventilation, passive cooling.

SYMBOLS

Latin symbols

A	m^2	cross-section of duct
c_a, c_e, c_s	J/K.kg	specific heat of air, envelope and storage material
C	-	weighted specific heat ratio between total packed-bed and interstitial air
d_e	m	thickness of envelope
h	$W/K.m^2$	amplitude-dampening coefficient
h_0	$W/K.m^2$	convective exchange coefficient
$\Delta h, \Delta h_e$	$W/K.m^2$	additional amplitude-dampening coefficients due to storage in envelope
$\Delta \bar{h}, \Delta \bar{h}_e$	$W/K.m^2$	additional dampening coefficients due to average temperature differential
k	$W/K.m^2$	phase-shifting coefficient
k_0	$W/K.m^2$	periodic storage capacity of storage element
$\Delta k, \Delta k_e$	$W/K.m^2$	Additional phase-shifting coefficients due to storage in envelope
$\dot{m}_a$	kg/s	airflow

r	m	distance perpendicular to airflow (from envelope inner towards outer surface)
r_e, r_s	m	thickness of envelope and of storage element
s, s_e	m^2/m	exchange surface per unit length of packed bed and envelope
S, S_e	m^2	total exchange surface of packed bed and envelope
S_s	m^2	exchange surface of one storage element
t	s	time
T_a, T_e, T_s	°C	temperature of air, envelope and storage material
v, v_0	m/s	interstitial and free air velocity
V, V_s	m^3	volume of total packed bed and of one storage element
x	m	length
x_π	m	length at total phase-shift, general case
$x_{\pi 0}, x_{\pi \infty}$	m	length at total phase-shift, no and infinite convective exchange

Greek symbols

δ_e, δ_s	m	heat penetration depth of envelope and of storage material
ε	--	amplitude-transmission
ε_π	--	amplitude-transmission at total phase-shift, general case
$\varepsilon_{\pi 0}, \varepsilon_{\pi \infty}$	--	amplitude-transmission at total phase-shift, no and infinite convective exchange
φ	rad	phase-shift
η	--	void fraction
λ_e, λ_s	W/K.m	thermal conductivity of envelope and of storage material
θ_0, θ_e	K	input temperature amplitude and average differential to outer surface of envelope
ρ_a, ρ_e, ρ_s	kg/m^3	density of air, envelope and storage material
τ	s	period of temperature oscillation
ω	rad/s	frequency of temperature oscillation

1. INTRODUCTION

The phenomenon we are interested in was first discovered by way of an analytical study on so called air/soil heat exchangers or buried pipe systems [1], which are usually set up for dampening of the daily or annual meteorological oscillation carried by a ventilation system. To the contrary of latter systems, it was then theoretically and experimentally established, that it is possible to use piled up thin slabs so as to delay or phase-shift the thermal input signal, almost without dampening it out. At that time the exact nature of the phenomenon however wasn't known by the authors, nor was the possibility of optimization by way of other geometries than the ones used for the first trials.

Because of their high exchange surface, so called packed beds, which are composed of solid elements and a fluid flowing in the interstitial space among them, have been used for a long time in a variety of industrial processes, for thermal, mass or chemical transfers. Thermal applications, which are the ones

we are interested in, have themselves led to a vast literature, of which an extensive review was done by Wakao and Kaguei [2]. An overview of this literature yet seems to show that the controlled phase-shifting effect put forward here had never been evidenced before.

The analytical models developed so far are almost always used in the case of a one-shot excitation (heat storage with incoming air at constant temperature and initially thermalized packed-bed). That is the case in particular for one of the simplest of these models, the Schumann or two-phase model developed in 1929 [3], which usually serves as a reference for more elaborated models. As will be seen in this article, solution of the Schumann model in harmonic mode yields a straight forward explanation of the controlled phase-shifting phenomena we are interested in, as well as a powerful tool for analysis of experimental results.

2. ANALYTICAL MODEL

2.1 System description

The physical phenomenon under consideration takes place in a thermal storage similar to a packed-bed (Fig. 1), submitted to an airflow with harmonic thermal input. The system is entirely defined by:

- Identical storage elements each of volume V_s and exchange surface S_s, homogeneously distributed within a duct of cross-section A and length x, with a void fraction η. The two first parameters yield the thickness r_s of the storage elements, independently of their geometry (spheres, slabs, cylinders, etc.):

$$r_s = \frac{V_s}{S_s} \tag{1}$$

  The latter ones yield the total net storage volume V, as well as the total and unitary exchange surface S and s:

$$V = (1-\eta)Ax \tag{2}$$

$$S = \frac{V}{V_s} S_s = (1-\eta)\frac{Ax}{r_s} \tag{3}$$

$$s = \frac{S}{x} = (1-\eta)\frac{A}{r_s} \tag{4}$$

- The specific heat and the density of storage elements and air, which determine the weighted specific heat ratio between total packed-bed and interstitial air:

$$C = \frac{(1-\eta)c_s\rho_s + \eta c_a\rho_a}{\eta c_a\rho_a} \tag{5}$$

- A constant airflow $\dot{m}_a$, which yields the free and interstitial velocities v_0 and v:

$$v_0 = \frac{\dot{m}_a}{A\rho_a} \tag{6}$$

$$v = \frac{\dot{m}_a}{\eta A\rho_a} = \frac{v_0}{\eta} \tag{7}$$

- A heat exchange coefficient h_0, which determines the convective heat exchange between the airflow and the packed bed.
- A harmonic air temperature input of period τ, which determines following unitary periodic storage capacity:

$$k_0 = \omega c_s \rho_s r_s = \frac{\pi c_s \rho_s r_s}{\frac{\tau}{2}} \tag{8}$$

Unless otherwise stated, we will moreover retain following assumptions:

- Storage elements are sufficiently small for their individual temperature to be regarded as homogeneous (no intra-element temperature gradient).
- Repartition of storage elements and airflow on a cross-section is homogenous, and duct is totally adiabatic (no transversal temperature gradient and no thermal losses).
- Axial diffusion between storage elements is negligible in comparison to convective heat exchange between air and storage elements.

Figure 1: System schematic.

2.2 Schumann model in harmonic regime

Foregoing assumptions lead to following two-phase model, which represents energy balance of airflow and of storage elements:

$$c_a \dot{m}_a \left(\frac{1}{v} \partial_t T_a + \partial_x T_a \right) + s h_0 \left(T_a - T_s \right) = 0 \tag{9}$$

$$r_s c_s \rho_s \partial_t T_s + h_0 \left(T_s - T_a \right) = 0 \tag{10}$$

Initially proposed by Schumann [3], this model is widely used as a reference for a “one-shot” excitation (energy storage in an initially thermalized packed-bed, with incoming air at a distinct and constant temperature). However, as far as we know, the model had up to now never been solved and analyzed for the case of a harmonic excitation, as proposed here:

$$T_a\big|_{x=0} = \theta_0 \cos(\omega t) \tag{11}$$

In permanent regime, the solution accounts for a reduced as well as delayed signal:

$$T_a = \theta_0 \exp\left(-\frac{hsx}{c_a \dot{m}_a}\right)\cos\left(\omega\left(t-\frac{x}{v}\right)-\frac{ksx}{c_a \dot{m}_a}\right) \tag{12}$$

with:

$$h = \frac{h_0 k_0^2}{h_0^2 + k_0^2} \tag{13}$$

$$k = \frac{h_0^2 k_0}{h_0^2 + k_0^2} \tag{14}$$

Accordingly to this solution and making use of further up definitions, phase-shift φ writes as:

$$\begin{aligned}\varphi &= \frac{\omega x}{v} + \frac{ksx}{c_a \dot{m}_a} \\ &= \frac{\omega x}{v}\left(\frac{C(h_0/k_0)^2 + 1}{(h_0/k_0)^2 + 1}\right)\end{aligned} \tag{15}$$

Complete phase-shift ($\varphi = \pi$) hence is reached at following system-length and with following amplitude transmission:

$$x_\pi = v\frac{\tau}{2}\left(\frac{(h_0/k_0)^2 + 1}{C(h_0/k_0)^2 + 1}\right) \tag{16}$$

$$\begin{aligned}\varepsilon_\pi &= \exp\left(-\frac{hsx_\pi}{c_a \dot{m}_a}\right) \\ &= \exp\left(-\pi\frac{k_0}{h_0}\frac{(C-1)(h_0/k_0)^2}{C(h_0/k_0)^2 + 1}\right)\end{aligned} \tag{17}$$

For a given storage material and void fraction, as defined by C, these relations are determined by the ratio h_0/k_0. We do in particular observe following limiting cases (Fig. 2):

- Without heat exchange between air and packed bed:

$$x_{\pi 0} = \lim_{h_0/k_0 \to 0} x_\pi = v\frac{\tau}{2} \tag{18}$$

$$\varepsilon_{\pi 0} = \lim_{h_0/k_0 \to 0} \varepsilon_\pi = 1 \tag{19}$$

  In this case the thermal oscillation is being completely carried by the air, moving at interstitial velocity v and yielding a thermal wave of length $x_{\pi 0}$.

- With perfect heat exchange between air and packed bed:

$$x_{\pi\infty} = \lim_{h_0/k_0 \to \infty} x_\pi = \frac{1}{C} v \frac{\tau}{2} \tag{20}$$

$$\varepsilon_{\pi\infty} = \lim_{h_0/k_0 \to \infty} \varepsilon_\pi = 1 \tag{21}$$

By perfect and weighted distribution between air and packed-bed, energy transport (temperature) is in this case dissociated from mass transport (air), yielding a reduced thermal wavelength $x_{\pi\infty}$

Obviously this phenomenon only is of interest in the common case of a fairly small void fraction and a storage material with a high heat capacity as compared to air ($C >> 1$). Controlled thermal phase-shifting then merely appears as a reduction of the natural thermal wave-length carried by the airflow. Not surprisingly, this interpretation corroborates the need of a good convective exchange and a small storage element size (large exchange surface, negligible intra-element gradient), so as to efficiently distribute the heat wave between the air and the packed-bed.

In this case, phase-shifting length and associated amplitude transmission write as:

$$\text{if } c_s \rho_s >> c_a \rho_a \text{ and } \eta << 1 \text{ then } \begin{cases} x_\pi \approx \left(1 + \dfrac{k_0^2}{h_0^2}\right) \dfrac{c_a \rho_a}{(1-\eta) c_s \rho_s} v_0 \dfrac{\tau}{2} \\ \varepsilon_\pi \approx \exp\left(-\dfrac{k_0}{h_0} \pi\right) \end{cases} \tag{22}$$

Two distinct regimes can then be distinguished (Fig. 3): if $h_0 > k_0$ phase-shifting is the predominant effect, with a more or less important amplitude transmission; if $h_0 < k_0$ amplitude-dampening is the predominant effect, with more or less but insignificant phase-shift.

Figure 2: Schematic energy and temperature transport, as distributed between air and packed-bed.

Figure 3: Amplitude-dampening and phase-shifting of harmonic temperature input ($c_s \rho_s >> c_a \rho_a$ and $\eta << 1$).

2.3 Non adiabatic duct

So as to take into account the effects of a non adiabatic duct, we now consider a refined model with convective heat exchange between air and duct coupled to heat diffusion through the duct envelope (thermal isolation). For simplification purposes, later heat diffusion will be considered only perpendicular to the airflow (r-axis) and for a plane geometry (rectangular duct, disregarding corner effects). The modified model now writes as:

$$c_a \dot{m}_a \left(\frac{1}{v} \partial_t T_a + \partial_x T_a \right) + s h_0 \left(T_a - T_s \right) + s_e h_0 \left(T_a - T_e \big|_{r=0} \right) = 0 \tag{23}$$

$$r_s c_s \rho_s \partial_t T_s + h_0 \left(T_s - T_a \right) = 0 \tag{24}$$

$$\lambda_e \left. \frac{\partial T_e}{\partial r} \right|_{r=0} + h_0 \left(T_a - T_e \big|_{r=0} \right) = 0 \tag{25}$$

$$\partial_t T_e - \frac{\lambda_e}{c_e \rho_e} \frac{\partial^2 T_e}{\partial^2 r} = 0 \tag{26}$$

Each equation of latter model represents a specific energy balance: (23) for the airflow; (24) for the storage elements; (25) for the duct (envelope inner surface); (26) for heat diffusion within the envelope.

We will consider a harmonic input with an average temperature distinct from the one imposed at the envelope outer surface, as given by following border conditions:

$$T_a \big|_{x=0} = \theta_e + \theta_0 \cos(\omega t) \tag{27}$$

$$T_e \big|_{r=r_e} = 0 \tag{28}$$

where r_e represents the envelope thickness.

In permanent regime, the solution accounts for dampening of the average temperature differential, as well as for a reduced and delayed harmonic signal:

$$T_a = \theta_e \exp\left(- \frac{s_e \Delta\bar{h} x}{c_a \dot{m}_a} \right) \quad + \quad \theta_0 \exp\left(- \frac{(sh + s_e \Delta h) x}{c_a \dot{m}_a} \right) \cos\left(\omega \left(t - \frac{x}{v} \right) - \frac{(sk + s_e \Delta k) x}{c_a \dot{m}_a} \right) \tag{29}$$

Dampening of the average temperature differential θ_e is driven by serial link of the convective air/duct exchange coefficient h_0 with the conductive exchange coefficient through the envelope $\Delta\bar{h}_e$:

$$\Delta\bar{h} = \frac{h_0 \Delta\bar{h}_e}{h_0 + \Delta\bar{h}_e} \tag{30}$$

$$\Delta\bar{h}_e = \frac{\lambda_e}{r_e} \tag{31}$$

As compared to the adiabatic packed bed discussed before, additional amplitude-dampening and phase-shifting of the harmonic signal θ_0 are driven by coefficients Δh and Δk. Calculation and discussion of latter coefficients is fully developed within a previous work concerning heat exchange between an airflow in an empty duct and its surrounding [1]. In complex notation, they write

as the decomposition in real and imaginary parts of the serial link between the convective exchange coefficient h_0 and diffusive coefficients Δh_e and Δk_e, which are proper to harmonic heat storage and discharge within the envelope:

$$\Delta h + i\Delta k = \frac{h_0\left(\Delta h_e + i\Delta k_e\right)}{h_0 + \left(\Delta h_e + i\Delta k_e\right)} \tag{32}$$

$$\Delta h_e + i\Delta k_e = (1+i)\frac{\lambda_e}{\delta_e}\frac{\cosh\left((1+i)\frac{r_e}{\delta_e}\right)}{\sinh\left((1+i)\frac{r_e}{\delta_e}\right)} \tag{33}$$

where δ_e corresponds to the standard penetration depth of the harmonic signal into the envelope material:

$$\delta_e = \sqrt{\frac{\lambda_e}{c_e \rho_e}\frac{\tau}{\pi}} \tag{34}$$

It can be shown [1] that for an envelope thickness r_e equivalent to or larger than δ_e, latter coefficients simplify to:

$$\text{if } r_e \geq \delta_e \text{ then } \Delta h_e \approx \Delta k_e \approx \frac{\lambda_e}{\delta_e} \tag{35}$$

Latter solution will not be discussed in more details here. Making reference to equation (29) it will only be stressed that the additional amplitude-dampening and phase-shifting due to the envelope actually corresponds to a perturbation effect, which diminishes when reducing the ratio between envelope exchange surface s_e and packed bed exchange surface S, i.e. when increasing the duct section.

2.4 Other perturbations

Other models, on which detailed information can be found in the complete report [4], allow for characterization of other perturbations, not taken into account by the Schumann model. The most important results are summarized here in terms of the absolute error on amplitude-transmission as well as of the relative error on system-length, at total phase-shift and as compared to the value yielded by the Schumann model:

- Heat diffusion within the storage elements has a reasonably small effect as long as the thickness of the storage elements is less than 20% of the intra-particle penetration depth (which depends only on the signal frequency and the particle thermal diffusivity).

$$\frac{r_s}{\delta_s} < 10\% \quad \Rightarrow \quad \begin{cases} \Delta\varepsilon_\pi < 4\% \\ \dfrac{\Delta x_\pi}{x_\pi} < 2\% \end{cases} \tag{36}$$

with:

$$\delta_s = \sqrt{\frac{\lambda_s}{c_s \rho_s} \frac{\tau}{\pi}} \tag{37}$$

- Axial or inter-particle heat diffusion has a reasonably small effect as long as the related penetration depth is less than 5% of the length for complete phase-shift:

$$\frac{\delta_s}{x_{\pi\infty}} < 5\% \quad \Rightarrow \quad \begin{cases} \Delta\varepsilon_\pi < 5\% \\ \dfrac{\Delta x_\pi}{x_\pi} < 3\% \end{cases} \tag{38}$$

- The potentially most important perturbation relates to non homogenous airflows, due to non homogenous geometries, which leads to mixing of non-uniformly phase-shifted thermal waves and consequent thermal interference, which may drastically diminish amplitude-transmission of the input signal.

Except for the last of them, for which further characterization needs yet to be done, preceding effects are not relevant for analysis of the experimental results to be discussed below. It should only be stressed that making use only of the simple Schumann model (possibly with a non adiabatic duct), corresponds to include all of these effects into the heat exchange coefficient h_0, which should then be seen as an effective overall value.

2.5 Daily versus annual phase-shifting

So as to get a grasp of the possible system dimension for complete phase-shifting of a daily or of an annual thermal oscillation, we now come back to the simple Schumann model (adiabatic duct), with infinite convective heat exchange. Table 1 shows the theoretical system length for an airflow with free velocity $v_0 = 500$ m^3/h per m^2 (0.14 m/s) and a packed-bed/air with specific heat ratio $c_s\rho_s / c_a\rho_a = 2000$.

Table 1: Length for total phase-shift (half a period) in function of void fraction, perfect convective exchange ($c_s\rho_s / c_a\rho_a = 2000$, $v_0 = 500$ m^3/h.m^2).

From this table it is clear that, although a seducing idea, phase-shifting of the annual oscillation would turn out difficult to realize, especially when taking into account the necessity of an adiabatic lateral envelope. We will hence concentrate on phase-shifting of the daily oscillation, essentially for summer

cooling of buildings in mild climates (diurnal temperature overshoots, with daily average within the comfort zone).

3. DEVELOPMENT OF PROTOTYPES

3.1 Experimental setup

The tested prototype consists of a 1 m long duct of 0.5 x 0.5 m cross section, with 20 cm expanded polystyrene for lateral thermal isolation, which was filled and tested with different storage materials. Previously, a duct with reduced cross section (0.82 x 0.31 m) was used for filling with ceramic spheres, available in limited quantity, as well as for some tests with gravel. Altogether, following storage materials were tested (Fig. 4 and Tab.2):

- Gravel of different sizes (4/8, 8/16 or 16/32 mm, as well as a heterogeneous mix ranging between approximately 4 and 32 mm), filled up in a bulk.
- Ceramic spheres of 10 et 30 mm diameter, of manual cement, clay and lime fabric, filled up in a bulk (10 mm) or piled up regularly (30 cm).
- Ceramic slabs of 15 x 31 cm basis and 2.5 cm thickness, piled up with 1 or 2 mm calibrated interstitial air gap.
- Perforated ceramic bricks of 25 x 12 x 6 cm, piled up with perforations oriented in the sense of the airflow.
- PVC tubes of 16/13 mm external/internal diameter filled with water, disposed in horizontal staggered rows, perpendicularly to the airflow (cross flow).

Figure 4: Prototype with different storage materials.

Table 2: Storage properties and derived optimum system length.

Experiments had a duration of 5 days each (+ 2 initial days so as to establish a permanent regime), and were carried out with diverse airflows (between 10 and 1000 m^3/h per m^2 cross section). At input, thermally stable air from the lab was heated up so as to yield a superposition of 4 sinus of respectively 24, 12, 8 and 6 h period, for simultaneous calibration of the model upon several frequencies.

3.2 Methodology

Analysis of monitoring results was carried out in four steps:

1) Breakdown of the monitored input and output temperatures in complete Fourier series.
2) For each frequency, computation of the Schumann model, taking into account thermal losses through the envelope (non-adiabatic model, eq. 29).

3) Determination of effective airflow $\dot{m}_a$ and convective heat exchange h_0 by way of non linear minimization of the quadratic error between monitored and modeled output signal (sum of all frequencies). For analysis purposes, $\dot{m}_a$ is then expressed in terms of free velocity v_0 (m^3/h per m^2 cross section).
4) For the monitoring data as well as for the calibrated model, accordingly to eq. 29, linear extrapolation to a length yielding a complete 12 h shift of the daily oscillation, and exponential extrapolation of the associated amplitude-transmission.
5) For the calibrated model, suppression of the effect due to the envelope (adiabatic model, eq. 12), corresponding to large enough duct section, yielding negligible boundary effects.

As pointed out before, first tests were carried out in a duct of reduced cross section, filled up with 30 mm ceramic spheres. In these tests, input air was heated up with a simple 24 h sinus (dynamic easier to visualize than the complex harmonic signal used further down) and airflow temperature monitored every 25 cm (Fig. 5, left). For each of the tested airflows, following observations can be made (Fig. 5 right and Tab. 3):

- Equidistant monitoring points confirm an exponential dampening amplitude-transmission and a linear phase-shift of the harmonic input signal. As expected for the realistic case of a non-adiabatic envelope, one furthermore observes a decreasing air temperature average, which drops towards the lab temperature average.
- The calibrated non-adiabatic model in all cases fits very well the monitoring data (as well for linear phase-shifting, as for exponential dampening of amplitude-transmission and of air-lab average temperature differential). Thanks to this good model calibration, extrapolation to a length yielding a complete 12 h shift remains coherent, discrepancy between model and monitoring remaining very low (Tab. 3).
- Suppression of the border effects (adiabatic model) results in almost unchanged phase-shifting, but in quite better amplitude-transmission.

Considered synthetically, latter extrapolated results bring about following comments on the system efficiency, as it relates to air flow and air velocity:

- As expected, system length for complete 12 h phase-shifting is directly proportional to air velocity, i.e. system volume is directly proportional to air flow (0.85 m^3 packed bed per 100 m^3/h airflow).
- Associated amplitude-transmissions (29 – 77 % in adiabatic mode) strongly depend on the air velocity, i.e. on the cross section associated to a given airflow. As a matter of fact, despite very low values relating to compact piling up (free velocity of 55 – 270 $m^3/h.m^2$, i.e. 1.5 – 7.4 cm/s), the calibrated convective exchange coefficient h_0 has a linear dependence on the air velocity (2.4 –

11.5 W/K.m^2 relatively to the sphere surface), in a very sensible range as compared to the sphere specific storage capacity k_0 (0.94 W/K.m^2).

Figure 5: Lab-test with 30 mm ceramic spheres and simple sinus input, diverse airflows. Left: dynamic over 3 days at regularly spaced monitoring points. Right: comparison of monitoring data (points) and non-adiabatic model (continuous lines), as well as extrapolation to adiabatic model (dashed lines): amplitude-transmission and phase-shift of harmonic signal, as well as dampening of average airflow-room differential.

Table 3: Tests with 30 mm ceramic spheres and simple sinus input.: 1) comparison of monitoring data and non-adiabatic model at prototype length; 2) extrapolation to a length yielding a 12 h shift of the daily oscillation; 3) suppression of the border effects due to the envelope (adiabatic model).

So as to limit the border effects due to the non adiabatic envelope, further tests were carried out in a duct with increased 0.5 x 0.5 m cross section. Other experimental improvement was the use of a complex harmonic signal, composed of 4 superposed sinus, with an amplitude of approximately 3.5 K each and periods of 24, 12, 8 and 6 h, which permits calibration of the model (determination of h_0) simultaneously upon several frequencies (each with a distinct k_0). As an example, the typical calibration procedure is depicted here for a specific case (PVC tubes filled with water, subject to 316 m^3/h.m^2 airflow), for which an excellent correspondence between model and monitoring is manifest over all 4 frequencies (Fig. 6).

Figure 6: Typical monitored and simulated response to combined 4-sinus input (in this case PVC tube filled with water, 316 m3/h.m2 airflow). a) dynamic of the complete signal; b) dynamic of the 24 h frequency, as obtained by Fourier analysis; c) frequency response (amplitude-transmission and phase-shift).

The degree of accuracy of this calibration and extrapolation procedure is finally examined by a synthetic view over all experimental sets (Fig. 7):

- In general terms, both extrapolated system-length and amplitude-transmission are very well reproduced by the non-adiabatic model. An overestimated amplitude-transmission by some 10% however appears in the case of the ceramic slabs and of water tubes, due to somewhat poorer calibration at 1 m prototype length, exacerbated at extrapolation by a factor 3 to 7 for complete phase-shift.

- As expected, noticeable border effects due to non-adiabatic envelope only appear in the case of the prototype with reduced cross section (used for ceramic spheres, as well as for some sets with gravel), where adiabatic and non-adiabatic model differ in terms of amplitude-transmission.

Figure 7: Extrapolated amplitude-transmission and system-length for 12 h phase-shift of the daily frequency. a) comparison between monitoring and non-adiabatic model; b) comparison between non-adiabatic and adiabatic model.

3.3 Result overview

Latter extrapolated results finally relate as follows to air flow and velocity (Fig. 8):

- Coherently with theory, system length for complete 12 h phase-shifting is directly proportional to air velocity, i.e. system volume is directly proportional to air flow, with a proportionality factor for each storage material given by Tab. 2 (order of magnitude of 1 m^3 packed bed per 100 m^3/h airflow).
- Effective value of convective heat exchange strongly depends on the air velocity, so that a decreasing airflow also implies a decreasing amplitude-transmission.
- In the case of the ceramic spheres, transmissions over 70% are reached for airflows of 200 $m^3/h.m^2$. If this material turns out to yield very good thermal results, it also is the most expensive one, at least in such small quantities (> 6'000 Euro/m^3).
- Use of a gravel bed certainly is the simplest and cheapest option (30 Euro/m^3), but reasonable results need a good control of granulometry. If certain setups yield transmissions over 50%, other trials turn out very deceiving, probably due to non homogenous airflows, implying interference of differently phase-shifted signals. At this stage a certain doubt remains for use of such a material, and a more detailed study on air distribution in non regular geometries might be necessary.
- Transmissions over 70% are also reached with ceramic slabs, however for airflows over 600 $m^3/h.m^2$ (over 4 m system length). In order to grant for homogenous airflows, such setups must however be realized carefully.
- Best results are obtained with the water tubes, as well in terms of system length (2.4 m for 400 $m^3/h.m^2$), due to the important heat capacity of water, as in terms of amplitude-transmission (over 80% for 400 $m^3/h.m^2$), probably due to system regularity and airflow homogeneity.

Figure 8: Extrapolated amplitude-transmission and system-length for 12 h phase-shift of the daily frequency, in function of free air velocity.

Pressure loss, which determines auxiliary electricity consumption for fans, remains generally low (below 50 Pa for a 12 h phase-shift), except for the slab geometry with a 1 mm gap (more than 100 Pa

for a 12 h phase-shift), as well as for the tube geometry with high airflows. In latter case, a comparison with a model by Zhukauskas for staggered cross flow tube exchangers, cited by Incropera and De Witt [5], gives following results (Fig. 9):

- Monitored pressure loss (for Reynolds number between 180 and 1650) is very well reproduced by the Zhukauskas model (valid for Reynolds number between 10^1 and 2 x 10^6) and remains below 100 Pa for free velocities below 400 $m^3/h.m^2$.
- On the contrary, convective heat exchange as given by the Zhukauskas model (with validity however restrained to Reynolds number between 10^3 and 2 x 10^5) strongly overestimates the observed calibrated values. For as low airflows as the ones used here, determination of amplitude transmission by way of lab testing hence seems inevitable.

Figure 9: Pressure loss and convective exchange coefficient for staggered tubes, comparison of monitored prototype with model by Zhukauskas.

4. SYSTEM DESIGN FOR PASSIVE COOLING OF BUILDINGS

Above calibrated models allow for system design of phase-shifting devices for passive cooling of buildings, by simulation of the system response for standard meteorological data for Geneva, as given in one hour step over one year and decomposed in terms of Fourier analysis.

An example is given here for day/night thermal phase shifting of a 100 m^3/h airflow, by way of a packed bed of PVC tubes filled with water, as defined above. Duct cross section is maintained at 50 x 50 cm (free velocity of 400 $m^3/h.m^2$), with 20 cm expanded polystyrene for lateral thermal isolation, and system length is fixed at 2.3 m, accordingly to Fig. 8. System response is computed by way of the non-adiabatic Schumann model (eq. 29), with $h_0 = 15.9$ W/K.m^2 as given by interpolation of the calibrated values at nearby monitored free velocity (yielding 83% amplitude-transmission at total phase-shift in adiabatic mode, 80% in non-adiabatic mode as used here).

For comparison, we also compute amplitude-dampening of the same airflow by way of an air/soil heat exchanger, using a complete analytical solution for convective air/pipe and diffusive pipe/soil heat exchange in harmonic mode [1]. The system under consideration consists of a 12 cm diameter pipe buried in a soil with same 50 x 50 cm cross section, subject to adiabatic border conditions (corresponding to a multi-layer array of pipes with 50 cm interaxial distance, buried underneath a building, i.e. in absence of meteorological disturbance from upper surface). With 1900 kJ/K.m3 capacity and 1.9 W/K conductivity, dampening of day/night amplitude to a residual 17% requires a 20 m system length.

Besides the advantage in size for the phase-shifting device, operating conditions on a typical summer week shows the altogether different behavior of both systems (Fig. 10). Whereas the buried pipe system allows for continuous ventilation at a stable temperature within the comfort zone, the phase-shifting device allows for delaying of the nightly cooling peaks for their use in the middle of the day, thereby however also shifting the warm daily peaks towards the middle the night. In stand-alone mode, the advantage of the phase-shifting device hence mainly goes for office buildings with occupation and ventilation limited to daytime, for the warm airflow at night to be evacuated back to ambient instead of being driven into the building. Alternatively, one may also consider a mixed strategy with ventilation from the phase-shifting device during the day, coupled to direct ventilation from ambient during the night, so as to take advantage of the ambient cooling peak twice a day. As for previous case, continuous 24/24h operation of the phase-shifting device for charge and discharge of the ambient oscillation however remains mandatory, with warm airflow at night evacuated back to ambient.

Fig. 10: Compared cross-section and operation over a typical summer week of two passive cooling ventilation techniques: buried pipe (top) and thermal phase-shifter (bottom).

5. CONCLUSIONS

This study can be summarized with following conclusions:

- The possibility of complete phase-shift (half a period delay) of a thermal wave carried by an airflow, almost without dampening, was confirmed as well theoretically as experimentally. We did not found any trace of this phenomenon in literature.
- The most immediate application concerns phase-shifting of the meteorological day-night oscillation, for passive cooling of buildings during daytime. Although quite tempting, phase-shifting of the annual oscillation would require a too important storage volume for such a device to be viable.
- A theoretical analysis shows that thermal phase-shifting basically resumes to a simple phenomenon, the point being to use the thermal inertia of the packed bed so as to slow down the natural wavelength carried by the airflow velocity. This however requires a good convective exchange between air and storage material, as well as thin storage layers. Potentially most striking problem could arise from an inhomogeneous airflow, which can induce important signal losses.
- On the experimental level, the development of lab prototypes confirms the possibility of complete phase-shifting of the 24 h oscillation, with an order of magnitude of 1 m^3 storage medium per 100 m^3/h airflow. Amplitude transmission may be as high as 80% for precise and regular geometries, but strongly diminishes in the case of inhomogeneous storage geometries, which probably induce inhomogeneous airflows.

- Comparison between experimental and theoretical results is very satisfying and proves a high mastery of the implied phenomena, so that it should now be possible to realize functional real-size installations.

ACKNOWLEDGEMENTS

We would like to acknowledge :

- The Swiss federal office of energy for financial support, and in particular Jean Christophe Hadorn for his encouragements and critical review of our work.
- Eric Pampaloni of the University of Geneva for his valuable help during design, construction and running of the experimental prototypes.
- The Tuilerie de Bardonnex, Geneva, who leant us different ceramic materials for the experimental tests.

REFERENCES

[1] Hollmuller P. (2003), Analytical characterisation of amplitude-dampening and phase-shifting in air/soil heat-exchangers. International Journal of Heat and Mass Transfer, Vol. 46, pp. 4303-4317.

[2] Wakao N. and Kagei S. (1982), Heat and mass transfer in packed beds. Gordon and Breach Science Publishers, p. 363.

[3] Schumann T.E.W. (1929), Heat transfer: a liquid flowing through a porous prism. J. Franklin Inst. 208, pp. 405-416.

[4] Hollmuller P., Lachal B., Zgraggen J.-M. (2004), Déphaseur thermique diffusif. CUEPE, Université de Genève, p. 98. (www.unige.ch/cuepe/html/biblio/detail.php?id=306).

[5] Zhukauskas A. (1972), Heat Transfer From Tubes in Cross Flow. Advances in Heat Transfer, Vol. 8, Academic. Press, New York, pp. 92-160. *Cited in*: Incropera F. and De Witt D., Fundamentals of heat and mass transfer, Third Edition, John Wiley & Sons, 1990.

Figure $1 : System schematic.

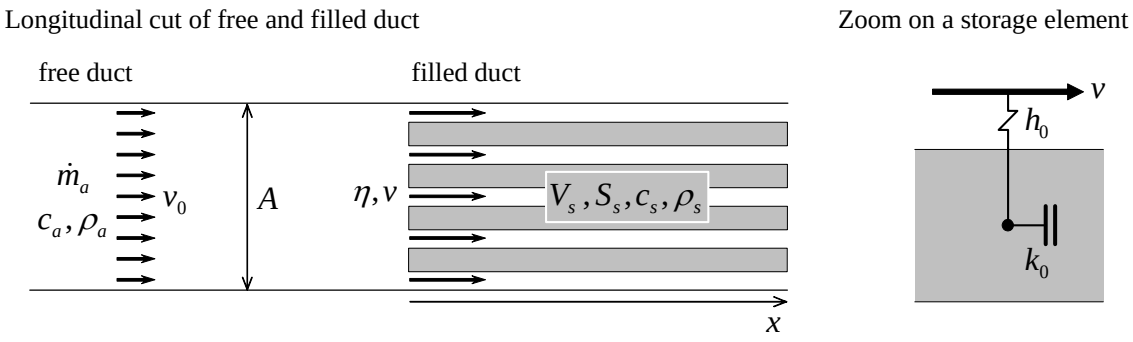

Figure $2 : Schematic energy and temperature transport, as distributed between air and packed-bed.

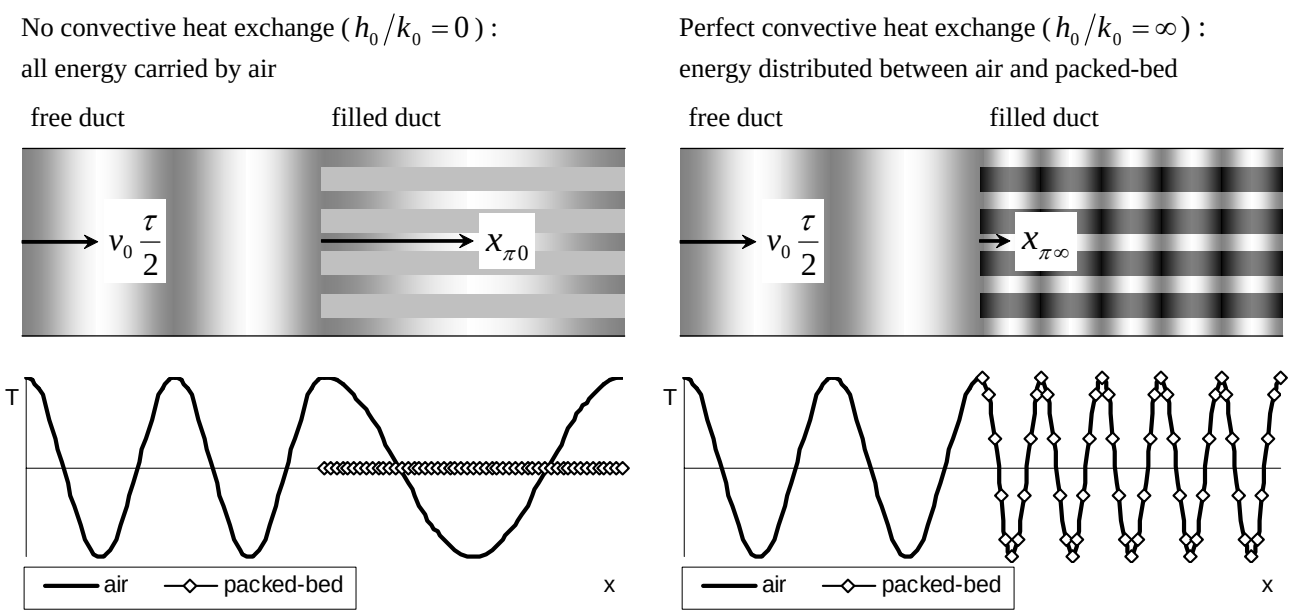

Figure $3 : Amplitude-dampening and phase-shifting of harmonic temperature input ($c_s\rho_s >> c_a\rho_a$ and $\eta << 1$).

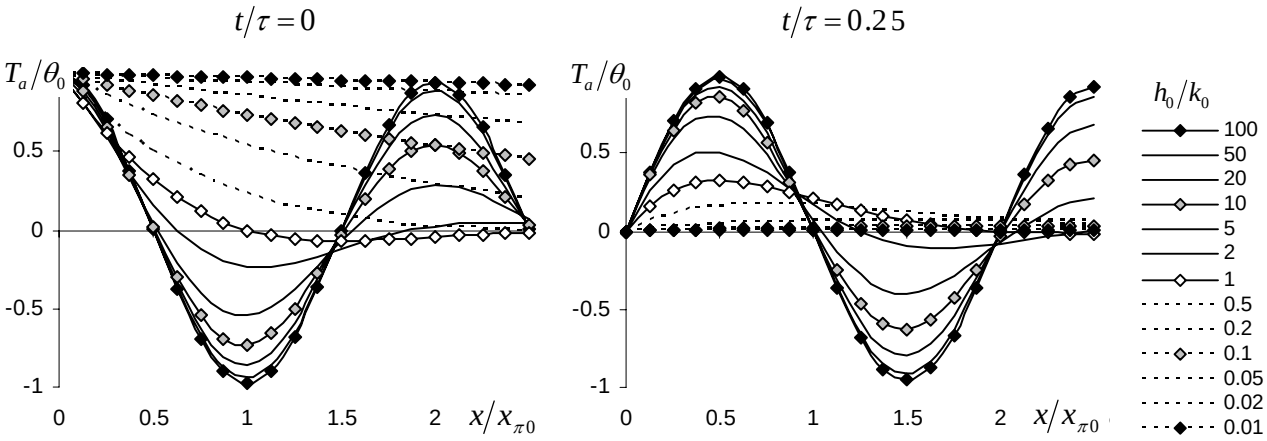

Figure $4 : Prototype filled with different storage materials. Top: ceramic spheres of two distinct sizes; Middle: gravel, perforated bricks; Bottom: ceramic slabs, pvc tubes filled with water.

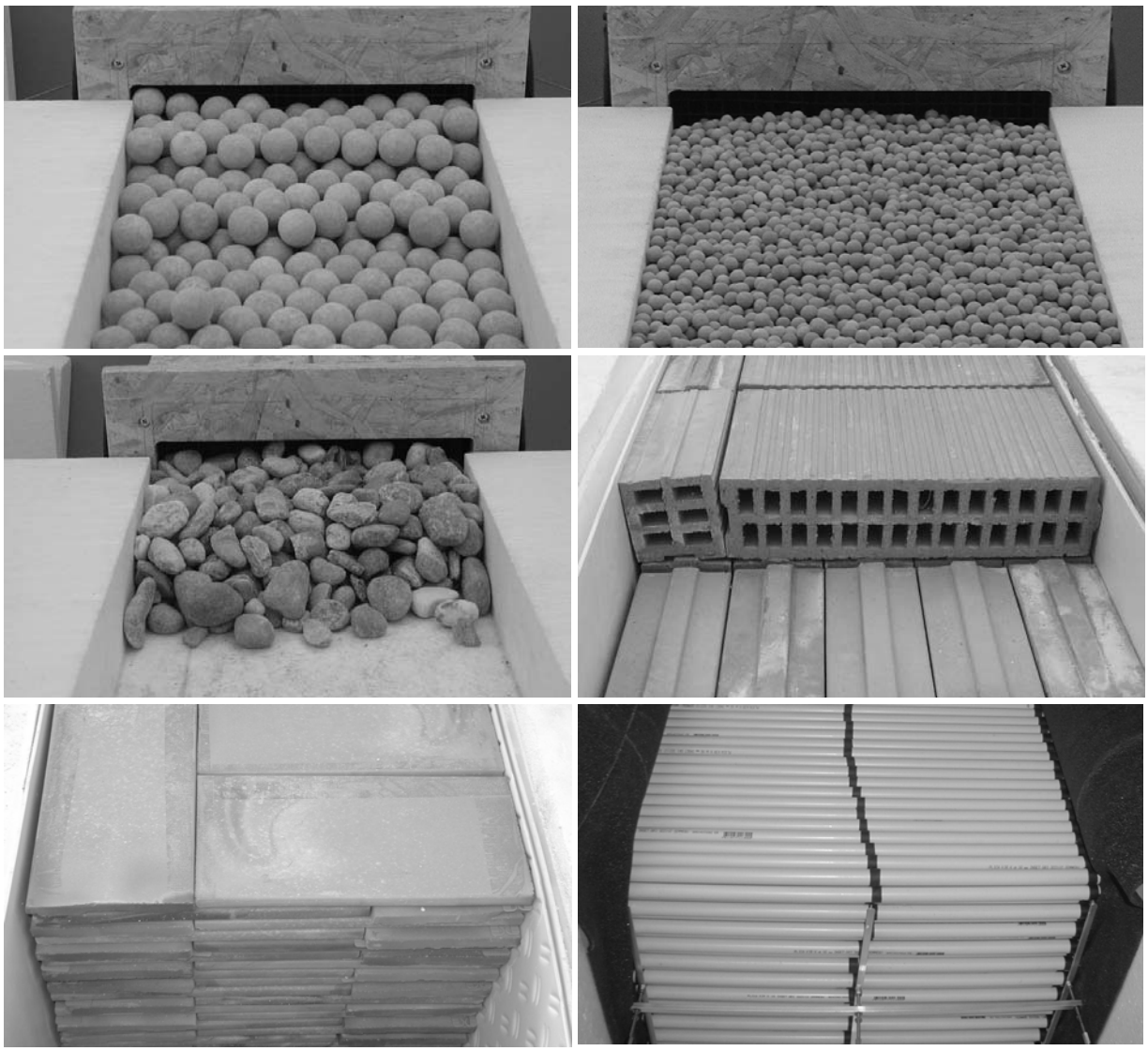

Figure $5 : Tests with 30 mm ceramic spheres and simple sinus input, diverse airflows. Left: dynamic over 3 days at regularly spaced monitoring points. Right: comparison of monitoring data (points) and non-adiabatic model (continuous lines), as well as extrapolation to adiabatic model (dashed lines): amplitude-transmission and phase-shift of harmonic signal, as well as dampening of average airflow-lab differential.

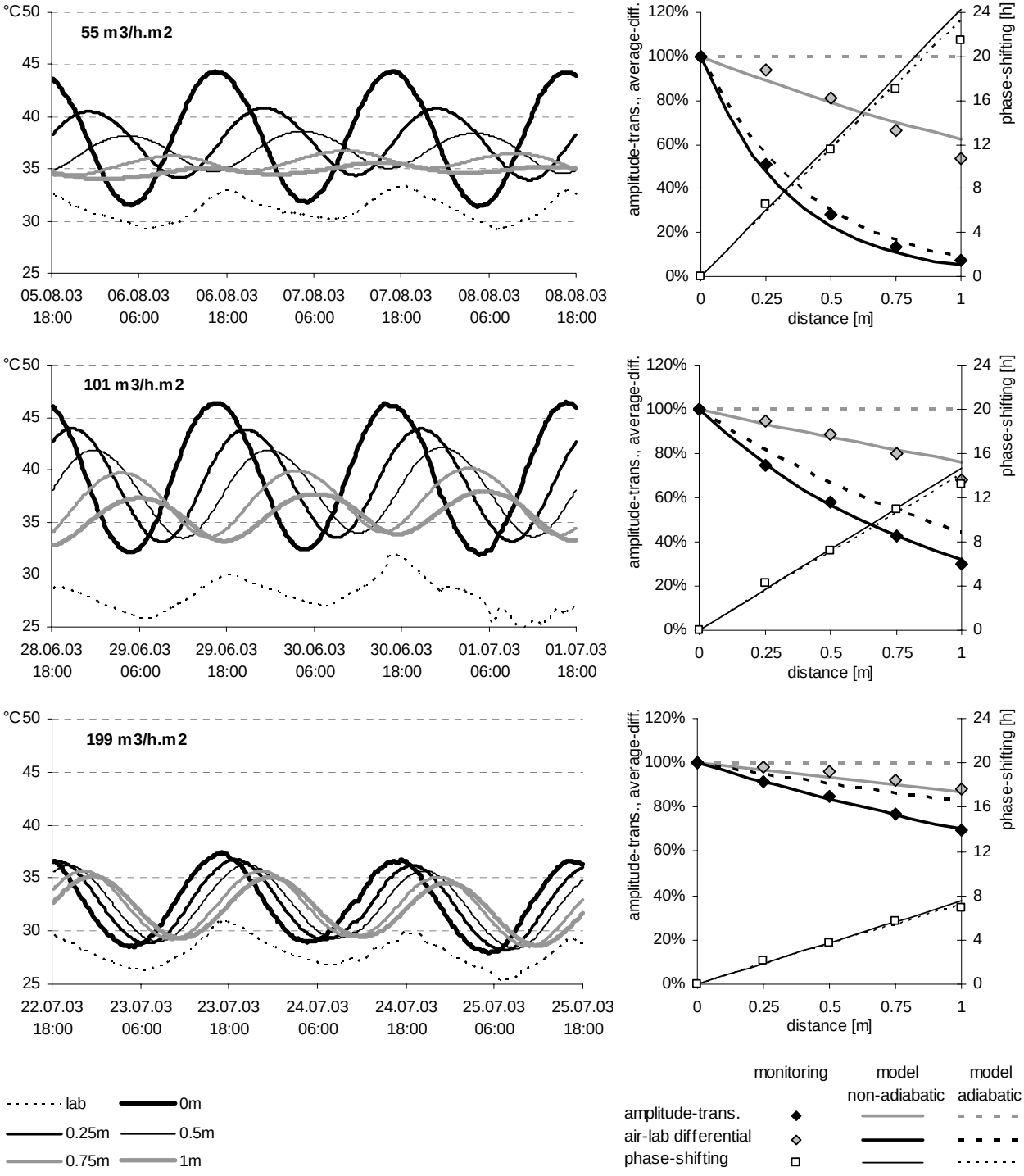

Figure $6 : Typical monitored and simulated response to combined 4-sinus input (in this case PVC tube filled with water, 316 $m^3/h.m^2$ airflow). a) dynamic of the complete signal; b) dynamic of the 24 h frequency, as obtained by Fourier analysis; c) frequency response (amplitude-transmission and phase-shift).

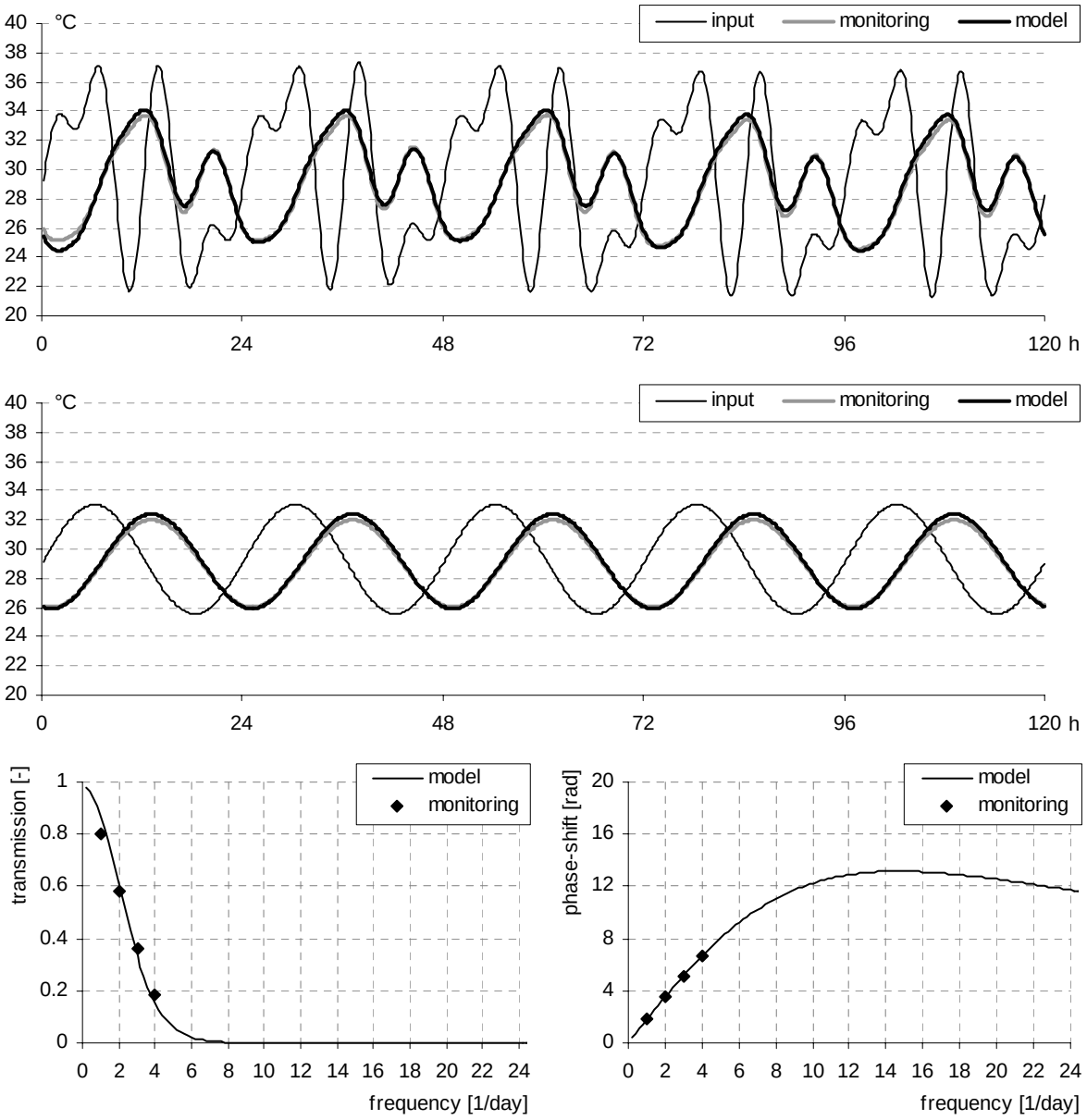

Figure $7 : Extrapolated amplitude-transmission and system-length for 12 h phase-shift of the daily frequency. a) comparison between monitoring and non-adiabatic model; b) comparison between non-adiabatic and adiabatic model.

Non-adiabatic model versus monitoring

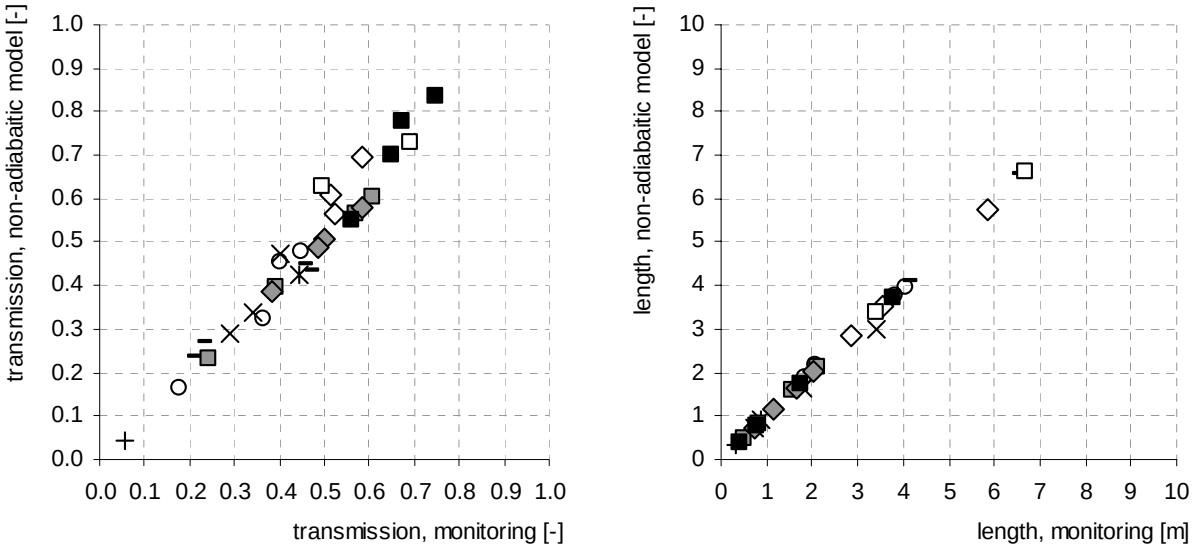

Adiabatic versus non-adiabatic model

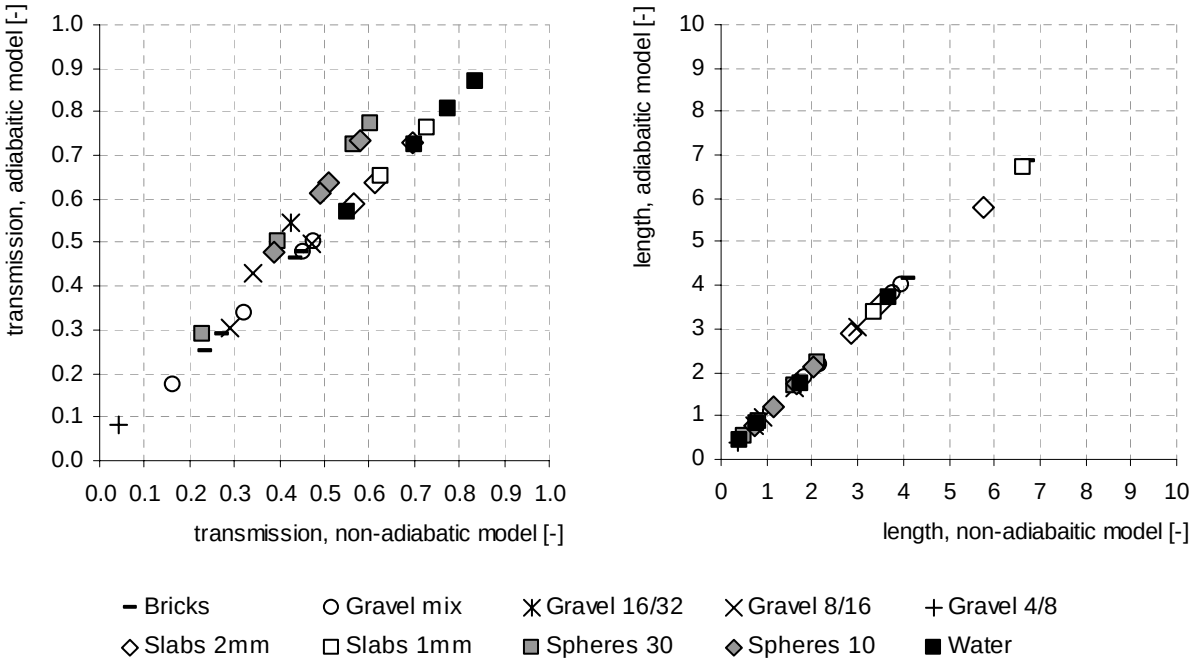

Figure $8 : Extrapolated amplitude-transmission and system-length for 12 h phase-shift of the daily frequency, in function of free air velocity.

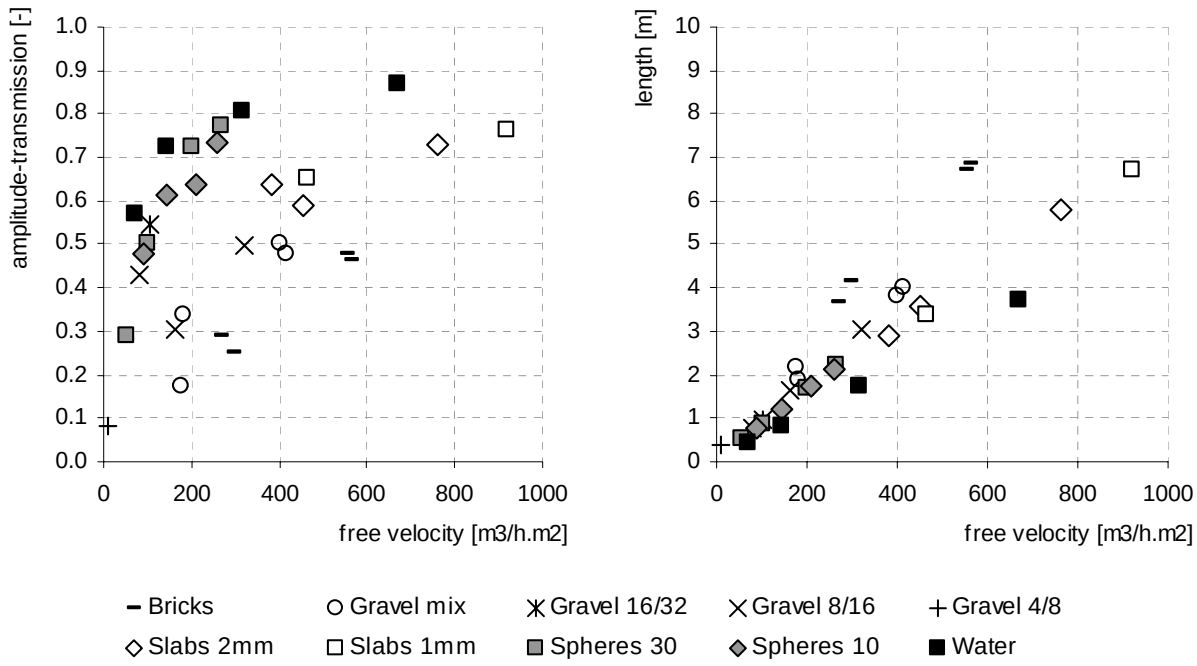

Figure $9 : Pressure loss and convective exchange coefficient for staggered tubes, comparison of monitored prototype with model by Zhukauskas.

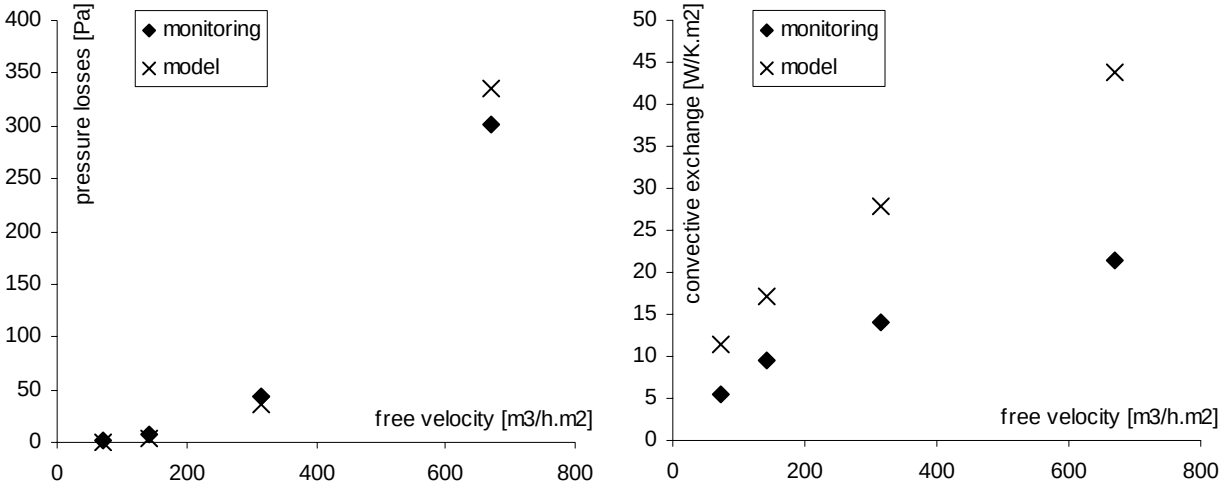

Figure $10 : Compared cross-section and operation over a typical summer week of two passive cooling ventilation techniques : buried pipe (top) and thermal phase-shifter (bottom).

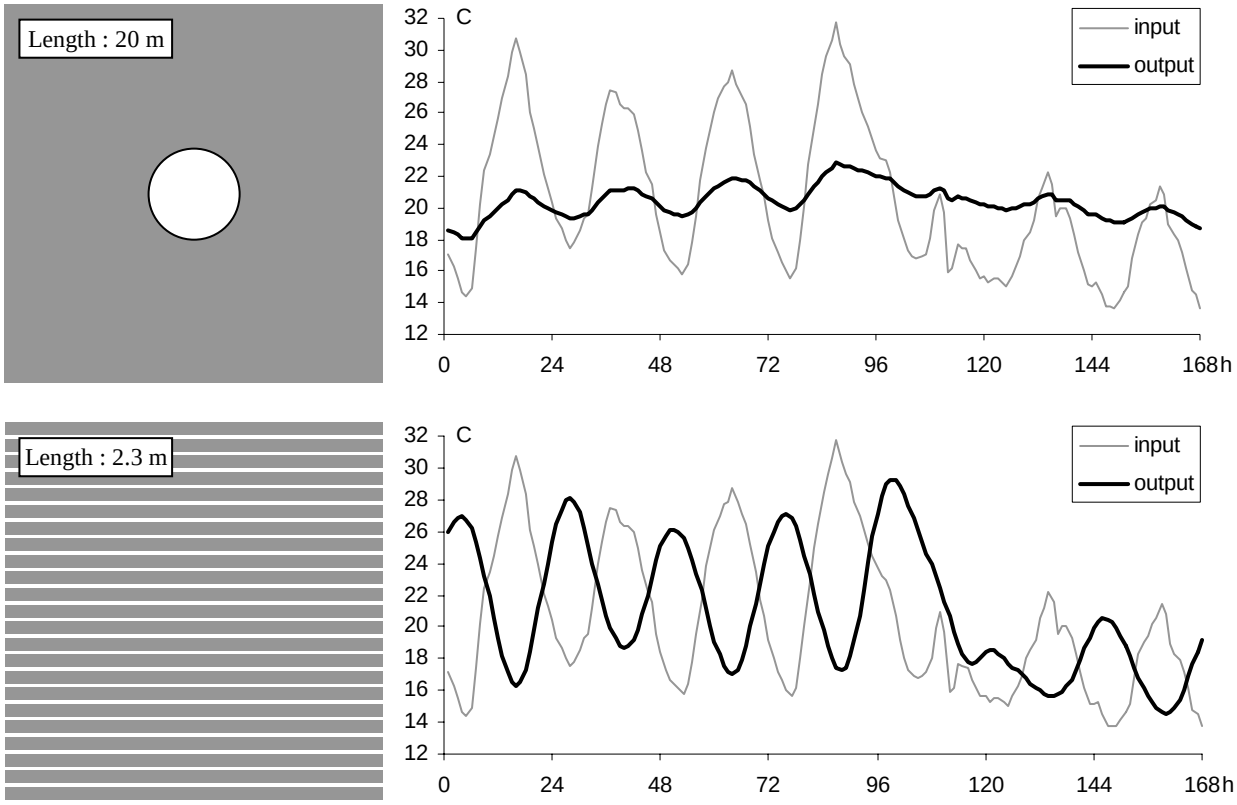

Table $1 : Length for total phase-shift (half a period) in function of void fraction, perfect convective exchange ($c_s\rho_s / c_a\rho_a = 2000$, $v_0 = 500\,\mathrm{m^3/h.m^2} = 0.139\,\mathrm{m/s}$).

η	v	$x_{\pi\infty}$ $\tau = 24\,h$	$x_{\pi\infty}$ $\tau = 365\,days$
	m/s	m	km
5%	2.78	3.16	1.15
10%	1.39	3.33	1.22
15%	0.93	3.53	1.29
20%	0.69	3.75	1.37
25%	0.56	4.00	1.46

Table $2 : Storage properties and derived optimum system length.

	c_s	ρ_s	$c_s\rho_s$	η	$\frac{x_{\pi\infty}}{v_0}$
	kJ/K.kg	kg/m^3	kJ/K.m^3		m per 100 m/h
Gravel	0.86	2620	2250	0.35	0.90
Ceramic spheres	1.10	2350	2580	0.39	0.84
Ceramic slabs 1mm gap	1.05	1820	1910	0.04	0.72
Ceramic slabs 2mm gap	1.05	1820	1910	0.07	0.74
Bricks	0.93	1890	1760	0.34	1.14
Water + PVC tube			3320	0.28	0.55

In the case of water and PVC tube, $c_s\rho_s$ represents the volumetric average.

Optimum system length is computed with $c_a\rho_a = 1.1$ kJ/K.m^3 (air at 30°C).

Table $3 : Tests with 30 mm ceramic spheres and simple sinus input: 1) comparison of monitoring data and non-adiabatic model at prototype length; 2) extrapolation to a length yielding a 12 h shift of the daily oscillation; 3) suppression of the effect due to the envelope (adiabatic model).

v_0	$m^3/h.m^2$	55	101	199	267
h_0	$W/K.m^2$	2.4	4.3	9.2	11.5
Prototype (1 m length)					
ε monitoring		7%	32%	70%	79%
ε model		5%	32%	70%	79%
φ monitoring	h	22.7	14.5	7.6	5.7
φ model	h	24.2	14.6	7.5	5.7
Extrapolation (12 h phase-shift)					
ε_π monitoring		24%	39%	57%	61%
ε_π model		23%	40%	57%	60%
x_π monitoring	m	0.53	0.83	1.58	2.10
x_π model	m	0.50	0.82	1.59	2.12
Extrapolation (12 h phase-shift) + adiabatic envelope					
ε_π model		29%	50%	73%	77%
x_π model	m	0.52	0.86	1.67	2.22